Pharm Res (2015) 32:2649–2662
DOI 10.1007/s11095-015-1650-1

RESEARCH PAPER

Endosomal pH-Responsive Polymer-Based Dual-Ligand-Modified Micellar Nanoparticles for Tumor Targeted Delivery and Facilitated Intracellular Release of Paclitaxel

Yajie Gao • Chao Zhang • Yanxia Zhou • Jinwen Li • Lei Zhao • Yushu Li • Yan Liu • Xinru Li

Received: 24 October 2014 / Accepted: 4 February 2015 / Published online: 13 February 2015

ABSTRACT

Purpose The purpose of the present study was to design and fabricate endosomal pH-sensitive dual-ligand-modified micellar nanoparticles to achieve enhanced drug delivery to tumor cells and facilitated intracellular drug release.

Methods End-group-carboxylated poly(2-ethyl-2-oxazoline)-poly(D,L-lactide) and cyclic Arg-Gly-Asp-Tyr-Lys- and anti-prostate specific membrane antigen antibody-modified diblock copolymer poly(2-ethyl-2-oxazoline)-poly(D,L-lactide) were synthesized and characterized by ^{1}H NMR and gel permeation chromatography, and self-assembled into micelles. Paclitaxel-loaded dual-ligand-modified micelles were prepared by thin-film hydration method, and characterized by dynamic light scattering, transmission electron microscope, pH-dependent *in vitro* release and stability. Intracellular paclitaxel delivery was measured by flow cytometry and imaged by confocal microscopy. *In vitro* cytotoxicity was studied in the 22Rv1 xenograft prostate tumor cell lines.

Results The prepared dual-ligand-modified micelles with about 30 nm in diameter and rapid intracellular drug release behavior at endo/lysosomal pH were very effective in enhancing the cytotoxicity of paclitaxel against 22Rv1 cells by increasing the cellular uptake, which was verified the correlation with the expression of integrin $\alpha_v\beta_3$ and prostate specific membrane antigen in tumor cells by flow cytometric analysis and confocal microscopy, compared with single ligand-modified micelles.

Conclusion These findings provided valuable information that the application of combining of dual-ligand modifications with pH-sensitivity to polymeric micelles may be a promising approach in the efficient delivery of anticancer drugs for treatment of integrin $\alpha_v\beta_3$ and prostate specific membrane antigen expressing prostate cancers.

Y. Gao • C. Zhang • Y. Zhou • J. Li • L. Zhao • Y. Li • Y. Liu (✉) • X. Li (✉)
Department of Pharmaceutics, School of Pharmaceutical Sciences, Peking University, Beijing 100191, China
e-mail: yanliu@bjmu.edu.cn
e-mail: ll@bjmu.edu.cn

KEY WORDS integrin $\alpha_v\beta_3$ · paclitaxel · pH-responsive polymeric micelles · prostate specific membrane antigen · tumor-targeting

INTRODUCTION

Cancer remains a major threat to public health. Chemotherapy is a type of cancer treatment that uses drugs to kill cancer cells. Therefore, efficient delivery of a threshold amount of antitumor drugs is required for successful therapy of cancer. Polymeric micelles (PM) have been demonstrated as one of the most promising nanocarriers for drug delivery (1, 2). They have presented great potential to improve water solubility of anticancer drugs, to prolong their blood circulation time, and to enhance their accumulation at tumor sites by enhanced permeability and retention (EPR) effect (3). However, the efficiency of passive targeting to tumor by EPR effect is limited.

To overcome this obstacle, tumor targeting ligands, such as small targeting molecule (4), oligopeptide (5), and antibody (6), have been anchored on the surface of nanocarriers to enhance their tumor cell targeting. These decorations of nanocarrier surface have been demonstrated to promote targeted delivery of drugs to tumor sites and improve their cellular uptake through specific binding between targeting ligands on nanocarrier surface and their specific receptors on tumor cell surface (7). However, most receptors are not exclusively expressed on tumor cells but also on some normal cells, and high affinity of targeted nanocarriers may lead to non-desired accumulation in regions of the body associated with low expression (8). Fortunately, tumor cell surface typically overexpresses multiple receptors. Efforts have been made to use dual-ligand targeting approach to enhance the tumor targeting specificity (9, 10). Herein, we focused on anti-

PSMA (prostate specific membrane antigen) antibody YPSMA-1 and cyclic Arg-Gly-Asp-Tyr-Lys (cRGDyK) as candidate ligands. PSMA, a classic type-II glycosylated transmembrane protein, is overexpressed in some primary and metastatic prostate cancer cells, such as 22Rv1 cells, and the tumor neovasculature (11–13). Its expression is independent of androgen, and upregulated after chemotherapeutics or surgical ablation therapy (14) and with disease progression (15). Several studies demonstrated that YPSMA-1-modified vehicles, such as liposomes (12, 16), could efficiently home to PSMA-expressing tumor cells and xenografts, and enhance therapeutic efficacy. However, PSMA is not expressed in some prostate cancer cells, such as PC-3 cells. cRGDyK exhibits high affinity to integrin $\alpha_v\beta_3$, a tumor angiogenesis biomarker that is overexpressed in tumor neovasculature and tumor cells but also on blood platelets, endotheliocytes. Previous documents reported that cRGDyK-conjugated nanocarriers facilitated their internalization into tumor cells via integrin-mediated endocytosis, displayed higher cytotoxicity and antiproliferation activities against tumor cells (17–20).

Notably, a great concern is that slow release of anticancer drug from PM in tumor cells may result in lower level of intracellular free drug and thereby limited antitumor efficacy (1, 21). Even worse, maintaining a lower level of intracellular free drug for a long time may lead to occurrence of drug resistance for tumor cells. Consequently, to guarantee the delivery of anticancer drug to tumor site and sufficient drug concentration for optimal efficacy and reduce side effects, PM is required to remain stable in the blood circulation and rapid release drugs to cytoplasm in tumor cells. This might be achieved by using targeted PM with a triggered release mechanism which enables the nanocarriers to release their cargos in response to the stimuli of tumor intracellular compartment, such as pH or enzymes (22, 23). On the other hand, ligand-modified nanocarriers are generally entrapped in endosomes after being internalized into tumor cells via an endocytic pathway, and finally delivered into acidic lysosomes, thereby leading to an inferior antitumor efficacy due to the degradation of the cargos by the lysosome enzymes (24). Therefore, it is very important to facilitate drug escape from endo/lysosome vesicles (25, 26). pH-responsive PM appeared to be the most attractive candidate due to the fact that the internalized micelles experienced a pH gradient from 5.5 to 6.5 in endosomes to 4.5–5.0 in lysosomes in their intracellular trafficking pathway.

In order to integrate the merits of dual-ligand-modified PM for enhancing accumulation at tumor sites and promoting uptake by tumor cells, and pH-sensitive PM for quick drug release in tumor cells and efficient endo/lysosome escape, we designed dual-ligand-modified pH-sensitive PM based on both cRGDyK- and YPSMA-1-conjugated pH-sensitive diblock copolymer poly(2-ethyl-2-oxazoline)-poly(D,L-lactide) (PEOz-PLA). A schematic diagram depicting the formation of multifunctional micelles and the intracellular trafficking was shown in Fig. 1. We hypothesized that PM would be endued with tumor cell-targeting ability and pH-response to intracellular compartments. Therefore, the physicochemical properties, pH-dependent *in vitro* release, and *in vitro* cytotoxicity against 22Rv1 cells and cellular uptake of micelles were all investigated in detail. The designed micelles were expected to be an effective delivery system for anticancer drugs to treat prostate cancers.

MATERIALS AND METHODS

Materials

Paclitaxel (PTX) was purchased from Guilin Huiang Biopharmaceutical Co. Ltd. (Guilin, China). cRGDyK was supplied by Shanghai C-Strong Co., Ltd. (Shanghai, China). YPSMA-1 was provided by Abcam (Cambridge, UK). 2-ethyl-2-oxazoline supplied by Sigma-Aldrich (St Louis, MO, USA) was dried by vacuum distillation over calcium hydride. D,L-lactide purchased from Daigang Biological Technology Co. Ltd. (Jinan, China) was purified by recrystallization from ethyl acetate. Ethyl 3-bromopropionate and stannous octoate were products of Aladdin reagent company (Shanghai, China). N-hydroxysuccinimide (NHS) and N-(3-dimethylaminopropyl)-N′-ethylcarbodiimide hydrochloride (EDC·HCl) were obtained from J&K scientific Ltd. (Beijing, China). Sulforhodamine B sodium salt (SRB) and coumarin-6 (donated as C6) were purchased from Sigma-Aldrich (St Louis, MO, USA). Bis Benzimide Hoechst 33258 was supplied by Biodee Biotechnology Co. Ltd. (Beijing, China). 3,3-dioctadecyl oxacarbocyanine perchlorate (DiO) and 1,1-dioctadecyl-3,3,30,30-tetramethylindocarbocyanine perchlorate (DiI) were purchased from J&K Chemical Ltd. (Shanghai, China).

Synthesis of End-Group-Carboxylated PEOz-PLA

End-group-carboxylated PEOz-PLA (HOOC-PEOz-PLA) diblock copolymer was synthesized using a two-step reaction procedure (Fig. 2a). HOOC-PEOz-OH was first synthesized by cationic ring-opening polymerization of 2-ethyl-2-oxazoline (25 g) using ethyl 3-bromopropionate (0.5 g) with 1.1 equiv of KI as initiators for 24 h in acetonitrile (50 mL) under nitrogen atmosphere and reflux condition, and then using 2.5 equiv of methanolic KOH as terminator followed by stirring for 12 h under reflux condition (27). The solvent was then removed from the reaction mixture by rotary evaporation. The crude product was dissolved in dichloromethane and precipitated in cold diethyl ether, and further purified by dialysis with a dialysis membrane (MWCO 3500, Millipore Co. Ltd, USA) against deionized water for 48 h. The dialysis solution was subsequently lyophilized to obtain the solid of HOOC-PEOz-OH with white color.

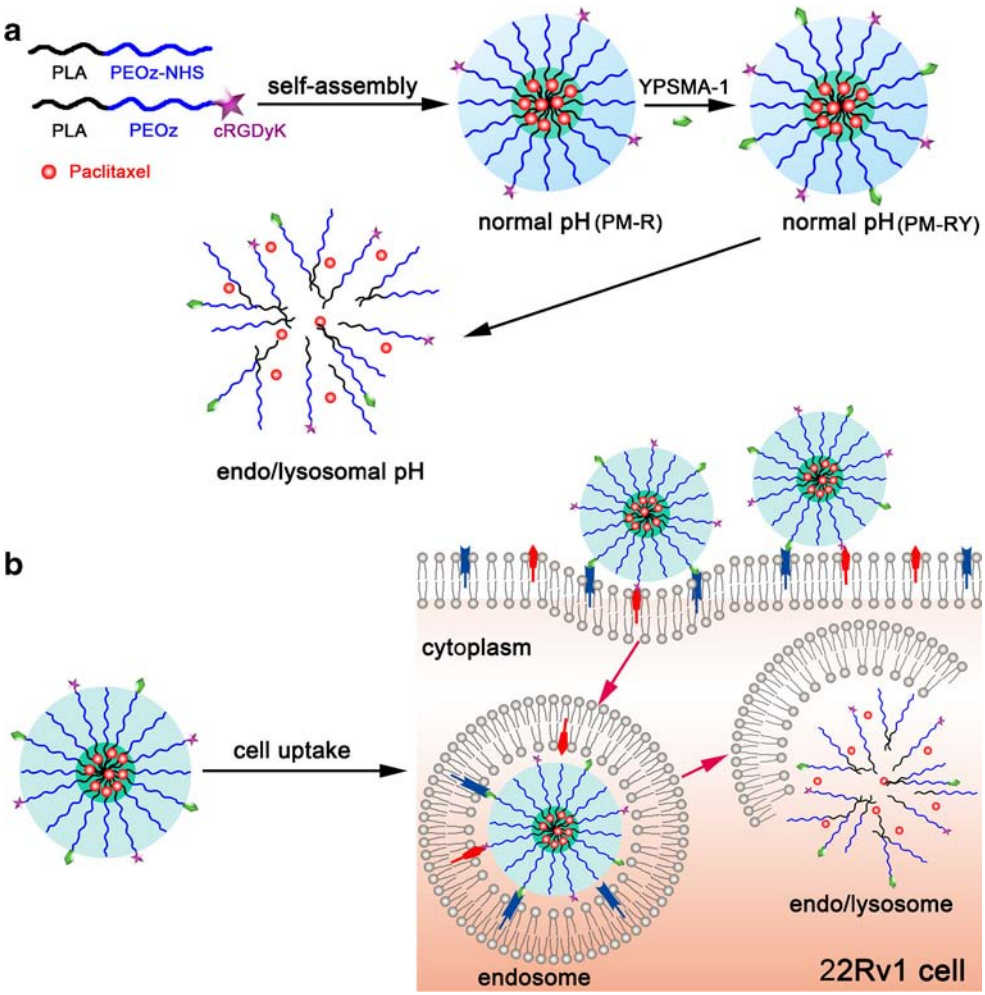

Fig. 1 (**a**) Schematic illustration of cRGDyK- and YPSMA-1-modified PEOz-PLA polymeric micelles and the acid-triggered drug release from micelles. (**b**) Schematic illustration of cellular uptake and intracellular trafficking of cRGDyK- and YPSMA-1-modified PEOz-PLA polymeric micelles in tumor cells.

The resulting HOOC-PEOz-OH was subsequently polymerized with D,L-lactide in toluene for 36 h under reflux condition using stannous octoate as the catalyst (28). The product was then obtained by precipitating in cold diethyl ether and drying under vacuum.

The polymers were characterized by ^{1}H NMR and gel permeation chromatography (GPC). The obtained polymers were dissolved in $CDCl_3$ and then ^{1}H NMR spectra were recorded on a Bruker MSL2300 spectrometer (400 MHz, Germany) using tetramethylsilane (TMS) as an internal reference at room temperature to characterize the chemical structure of the products. The molecular weight and molecular weight distribution were measured by GPC (Waters 1515) with a refractive index detector (Waters 2414) by using polystyrene as standards.

Synthesis and Characterization of NHS-PEOz-PLA

HOOC-PEOz-PLA, EDC·HCl (2 excess), NHS (2excess) and dichloromethane were added to a round-bottle flask equipped a magnetic stirring bar, purged with nitrogen atmosphere (Fig. 2b). The reaction was maintained for 24 h at room temperature. The reaction mixture was washed twice with saturated NaCl solution to remove the excessive NHS and EDC·HCl, then precipitated in cold diethyl ether and dried in vacuum to constant weight. The final product was characterized via ^{1}H NMR.

Synthesis of cRGDyK-PEOz-PLA

The cRGDyK was conjugated to the terminal of HOOC-PEOz-PLA using an EDC/NHS technique (29, 30) (Fig. 2b). In brief, NHS and EDC·HCl were added to HOOC-PEOz-PLA suspended in deionized water at a molar ratio of 2:2:1, and pH was adjusted to 5.0–6.0 with HCl solution under moderate stirring in ice bath. After 15 min of reaction, 1 equiv of cRGDyK was added and pH value was adjusted to 8.0–8.5. After the incubation maintained 24 h at room temperature, the resultant mixture was put into a dialysis bag (MWCO 3500, Millipore Co. Ltd, USA) and dialyzed against deionized water for 24 h to remove the residual EDC,

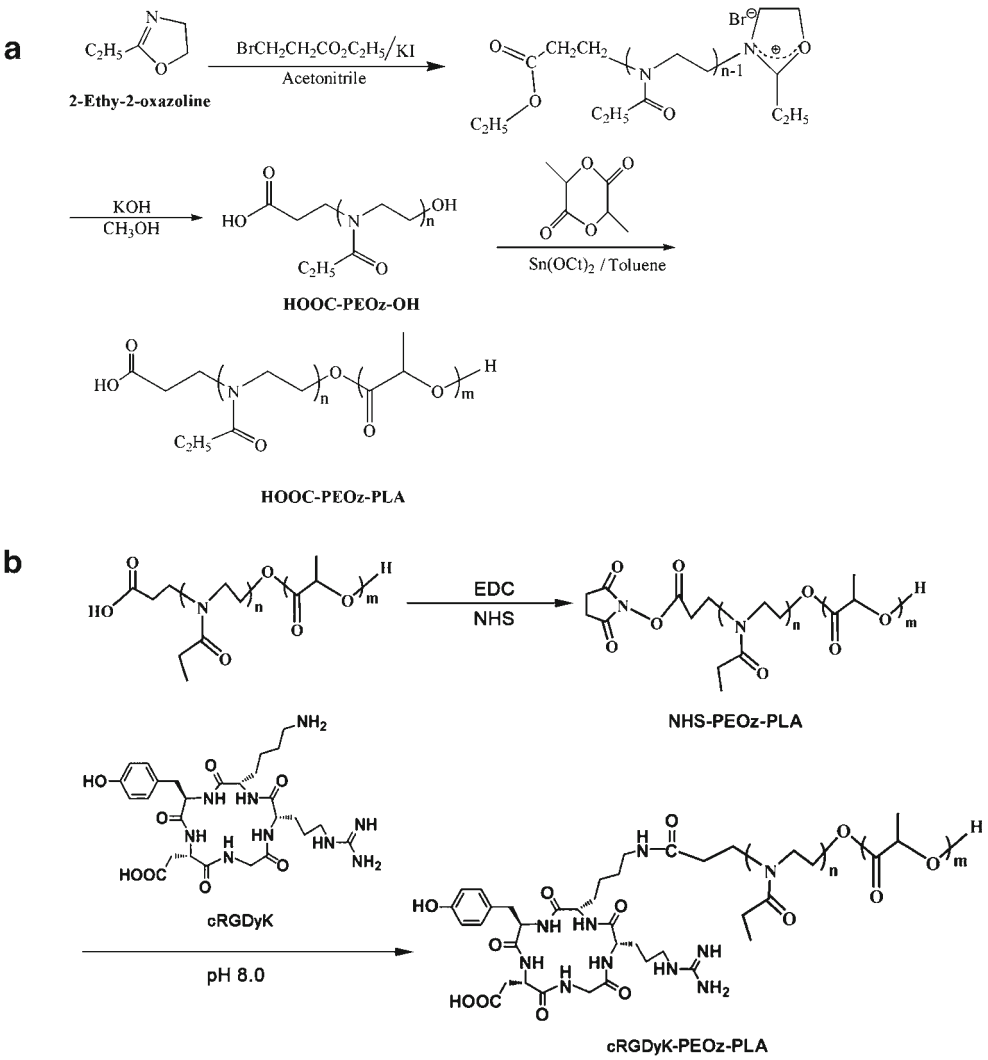

Fig. 2 Synthesis procedures of HOOC-PEOz-PLA (**a**), and NHS-PEOz-PLA and cRGDyK-PEOz-PLA (**b**).

NHS and cRGDyK. Then the dialysis solution was lyophilized and stored at −20°C until use.

Determination of Critical Micelle Concentration of HOOC-PEOz-PLA

The critical micelle concentration (CMC) of the copolymer was measured by a fluorescence technique with pyrene as a hydrophobic probe as described previously (31).

Preparation of Drug-Loaded PM

PTX-loaded PM (denoted as PTX/PM) was prepared by thin-film hydration method (32). In order to encapsulate large amount of PTX, the processing technique of PTX-loaded micelles was optimized in our preliminary test. Briefly, HOOC-PEOz-PLA (10 mg) and PTX (1 mg) were dissolved in 20 mL of methanol followed by evaporation under vacuum at 60°C to form a stripped film. The resultant thin film was hydrated with 5 mL of deionized water at 60°C and then vortexed for 5 min. Non-encapsulated paclitaxel was removed by filtration of the micelle suspensions through a 0.22 μm polycarbonate membrane (Millex-GV, Millipore, USA) to obtain a clear and homogeneous micelle solution.

For preparation of PTX-loaded PM modified with cRGDyK (denoted as PTX/PM-R), similar procedure was taken as described above except that HOOC-PEOz-PLA was replaced by a mixture of cRGDyK-PEOz-PLA and HOOC-PEOz-PLA (1:1, *w*/*w*).

For preparation of PTX-loaded PM modified with YPSMA-1 (denoted as PTX/PM-Y), NHS-PEOz-PLA, HOOC-PEOz-PLA and PTX (5:5:1, *w*/*w*/*w*) were dissolved in methanol, and then evaporated, hydrated, vortexed and filtered as described above to obtain N-hydroxysuccinimide-activated PTX/PM. The resultant micelle suspension was subsequently allowed to react with YPSMA-1 for 24 h under magnetic stirring. After which, the micelle suspension was subjected to a Sepharose CL-4B column and eluted with distilled water to remove the free YPSMA-1. The conjugation efficiency of YPSMA-1 was about 25% determined using the Micro BCA Protein kit.

For preparation of PTX-loaded PM modified with both cRGDyK and YPSMA-1(denoted as PTX/PM-RY) (Fig. 1a), NHS-PEOz-PLA, cRGDyK-PEOz-PLA and PTX (5:5:1, *w*/*w*/*w*) were dissolved in methanol, and then evaporated, hydrated, vortexed and filtered as described above to obtain N-hydroxysuccinimide-activated PTX/PM-R. The resultant micelle suspension was subsequently allowed to react with YPSMA-1 for 24 h under magnetic stirring. After which, the micelle suspension was subjected to a Sepharose CL-4B column and eluted with distilled water to remove the free YPSMA-1. The conjugation efficiency of YPSMA-1 was about 25% determined using the Micro BCA Protein kit.

C6-, DiI/DiO-loaded PM was prepared as described above. In the C6-loaded micelles, the C6/polymer ratio was 1:1000 (*w*/*w*); while in the (DiI/DiO)-loaded micelles (denoted as FRET micelles), the DiO/polymer and DiI/polymer ratio was 1:500 (*w*/*w*), respectively.

Physicochemical Characterization of PTX-Loaded PM

Size and size distribution, and Zeta potential of PM were determined by dynamic light scattering (DLS) using Malvern Zetasizer Nano ZS (Malvern, UK) with a scattering angle of 90° at 25°C after diluting the micelle solution to an appropriate volume with deionized water. The morphology of PMs was visualized by transmission electron microscope (TEM, JEM-1230, JEOL, Japan). Before examination, the sample was stained with a drop of 1 wt% phosphotungstic acid solution, and then placed on a copper grid with carbon film followed by removal of the excess fluid with filter paper, and dried for 48 h.

The encapsulation efficiency (EE) and loading content (LC) were determined as follows: a predetermined amount of lyophilized micelles was dissolved in methanol. The PTX level loaded in micelles was measured on a Agilent HPLC System (Agilent Technologies, CA, USA) equipped with a UV detector and a reverse phase (ODS C-18, 250×4.6 mm, 5 μm, Diamobsil, China). The mobile phase consisted of methanol, acetonitrile and water (37.5:37.5:25, *v*/*v*/*v*) and was pumped at flow rate of 1.0 mL/min. The column temperature was maintained at 25°C. The detection wavelength was set at 227 nm. The EE was defined as the ratio of the amount of PTX loaded in micelles to the original feeding amount of PTX. The LC was calculated as the percentage of the amount of PTX loaded in micelles over the amount of lyophilized micelles.

The *in vitro* release behavior of PTX from various PTX-loaded PM was monitored by using a dialysis-bag diffusion method as described previously with little modification (33). Briefly, 1 mL of PTX-loaded micelle solution was introduced into a dialysis bag (MWCO 3500), and the sealed dialysis bag was completely submerged into 50 mL of PBS (pH 5.0, 7.4) with 0.5% Tween 80 at 37°C and 100 rpm. At predetermined time points (1, 4, 8, 12, 24 h), 1 mL of the release medium was withdrawn and replaced with equal volume of fresh media. The concentration of released PTX in medium was measured by HPLC method as described above and the accumulative release amount (%) was calculated.

Physicochemical Characterization of C6- and DiI/DiO-Loaded PM

Size and size distribution of PM were determined as described earlier.

The encapsulation efficiency (EE) was determined as described above. The amount of C6 or DiI/DiO loaded in micelles was quantified by using a fluorospectrophotometer (Shimadzu, RF-5301, Japan) operating at excitation wavelength of 488 nm and emission wavelength of 521 nm for C6, excitation wavelength of 549 nm and emission wavelength of 565 nm for DiI, excitation wavelength of 484 nm and emission wavelength of 501 nm for DiO, respectively.

The *in vitro* leakage of C6 from PM against serum-free medium (pH 7.4) under continuous gentle shaking at 37°C (100 rpm) was evaluated using a dialysis diffusion method as described above. The cut-off molecular weight of the dialysis bag was 3500 Da. The concentration of leaked C6 in the medium was measured by fluorescence spectrophotometry method as described above and the accumulative leakage amount (%) was calculated.

Cell Culture

22Rv1 cells were obtained from Cell Culture Center of Institute of Basic Medical Sciences, Chinese Academy of Medical Sciences and Peking Union Medical College (Beijing, China). Cells were cultured in RPMI 1640 medium (MAC Gene Technology) supplemented with 10% fetal bovine serum (FBS, Gibco) and 1% Penicillin-Streptomycin in 5% CO_2 humidified atmosphere at 37°C, and subcultivated every 3–4 days at 80–90% confluence and digested with Trypsin–EDTA (MAC Gene Technology, Beijing, China) at a split ratio of 1:3.

Stability of PM After Contacting with Cells

The stability of the micelles was evaluated through the release of core-loaded molecules from micelles by using the Förster resonance energy transfer (FRET) method when they were in contact with 22Rv1 cells (34). Briefly, 22Rv1 cells were seeded on a glass bottom culture dish (35-mm dish with 20-mm glass bottom well) and cultured at 37°C under 5% CO_2 for adherence. After the cells were subcultivated at 80–90% confluence, the culture media were removed, and the cells were washed with serum-free medium at 37°C for three times. Subsequently, the medium containing FRET micelles (final concentration

of both DiI and DiO was 4 μg/mL) was added. After 0.5 h incubation, the cells were immediately put on the microscope stage of CLSM, and FRET images were obtained with a confocal laser scanning microscope (CLSM, TCS SP5, Leica, Germany). The excitation and emission wavelengths for DiO were 484 nm and 500–530 nm, respectively, and 549 nm and 555–655 nm for DiI, respectively. For determination of FRET, the excitation wavelength (484 nm) of DiO as the donor and the emission wavelength (555–655 nm) of DiI as the acceptor were used, respectively.

Cytotoxicity Assessment

The SRB assay was applied to investigate the *in vitro* cytotoxicity of various PTX-loaded PM on 22Rv1 cells (28, 35). In brief, 22Rv1 cells were seeded in 96-well plates at a density of 1×10^4 cells/well and cultured at 37°C in 5% CO_2 humidified atmosphere for 24 h. Then the culture medium in each well was replaced with 200 μL of fresh medium containing free PTX, different micelle formulations with serial PTX concentration, respectively. The PTX-free culture medium was used as negative control. Cells were also treated with blank micelles with indicated HOOC-PEOz-PLA concentrations to evaluate the cytotoxicity of the vehicle. After incubation for further 72 h, cells were washed with cold PBS for three times and fixed with 200 μL of 10% trichloroacetic acid (TCA) for 1 h at 4°C, then washed 5 times with deionized water after removing TCA and dried in the air. The fixed cells were then stained with 100 μL of 0.4% SRB for 30 min and followed by washing 5 times with 1% acetic acid after removing SRB and drying at 37°C. The absorbance at 540 nm was determined using a microplate reader (BIO-RAD model 680, Shanghai, China) after the bound dye in each well was dissolved in 200 μL of 10 mM Tris. The cytotoxicity of tested samples was expressed as the ratio of the absorbance of the tested groups to that of the negative control.

Flow Cytometric Analysis

22Rv1 cells were seeded into 6-well plates (3×10^5 cells/well) and cultured for 24 h at 37°C under 5% CO_2. The medium was replaced by the medium containing free C6, C6/PM, C6/PM-R, C6/PM-Y and C6/PM-RY with a final C6 concentration of 100 ng/mL. After 4 h of incubation, the cells were washed thrice with cold PBS, trypsinized and harvested with 0.4 mL of 0.2% (*w*/*v*) trypsin-0.1% (*w*/*v*) EDTA solution, and resuspended in 0.5 mL of PBS followed by filtration through a nylon mesh. The C6 uptake in the cells was measured by FAScan flow cytometer (Becton Dickinson FACS Calibur, Mountain View, USA). For each sample, 10,000 events were collected and the data were analyzed.

To investigate whether cRGDyK and YPSMA-1 could hinder C6/PM-R and C6/PM-Y endocytosis, respectively, cells were pre-incubated with 0.5 μg/mL of free cRGDyK or 0.1 μg/mL of free YPSMA-1 for 30 min before they were exposed to C6/PM-R and C6/PM-Y, respectively.

Confocal Microscopy Observation

22Rv1 cells were cultured in glass-bottomed 24-well plates at a density of 1×10^5 cells/well for 24 h. The medium was replaced by the medium containing free C6, C6/PM, C6/PM-R, C6/PM-Y and C6/PM-RY with a final C6 concentration of 50 ng/mL, respectively. After another 1.5 h incubation, the medium was removed and cells were washed thrice with cold PBS followed by fixing with 4% paraformaldehyde at 37°C for 20 min and washing thrice with PBS. Then the fixed cells were stained with Hoechst 33258 for 15 min. The fluorescent images of the cells were visualized using confocal laser scanning microscope (CLSM, Leica, TCS SP2, Germany).

Statistical Analysis

Data are presented as mean ± standard deviation. One-way analysis of variance was used to determine the statistical significance of differences among multiple groups. A *p*-value of 0.05 or less was considered to be statistically significant.

RESULTS

Synthesis and Characterization of HOOC-PEOz-PLA Copolymer

As shown in Fig. 2a, HOOC-PEOz-OH was first synthesized by cationic ring-opening polymerization of EOz. The successful synthesis of HOOC-PEOz-OH was verified by ^{1}H NMR spectrum (Fig. 3a). The pendent peaks at 1.12 and 2.44 ppm were attributed to methyl (***CH*$_3$**CH_2CO-) and methylene (CH_3***CH*$_2$**CO-) protons in side chains, respectively. The peak at 3.49 ppm was assigned to methylene protons (−N***CH*$_2$*CH*$_2$**-N-) in the backbone. The number-average molecular weight (M_n) and molecular weight distribution of HOOC-PEOz-OH determined by GPC was 4338 g/mol with relatively low PDI of 1.16.

Then, HOOC-PEOz-PLA was synthesized by anionic ring-opening polymerization of HOOC-PEOz-OH and D, L-lactide using stannous octoate as the catalyst (Fig. 2a). The characteristic peaks corresponding to PLA (5.17 and 1.56 ppm) and PEOz (1.12, 2.44 and 3.49 ppm) were observed (Fig. 3b), which were in agreement with our previous report (28). The number-average molecular weight (M_n) of HOOC-PEOz-PLA determined by GPC was 7097 g/mol (PDI: 1.26).

The CMC of HOOC-PEOz-PLA was measured by a fluorescence spectrophotometer using pyrene as a hydrophobic

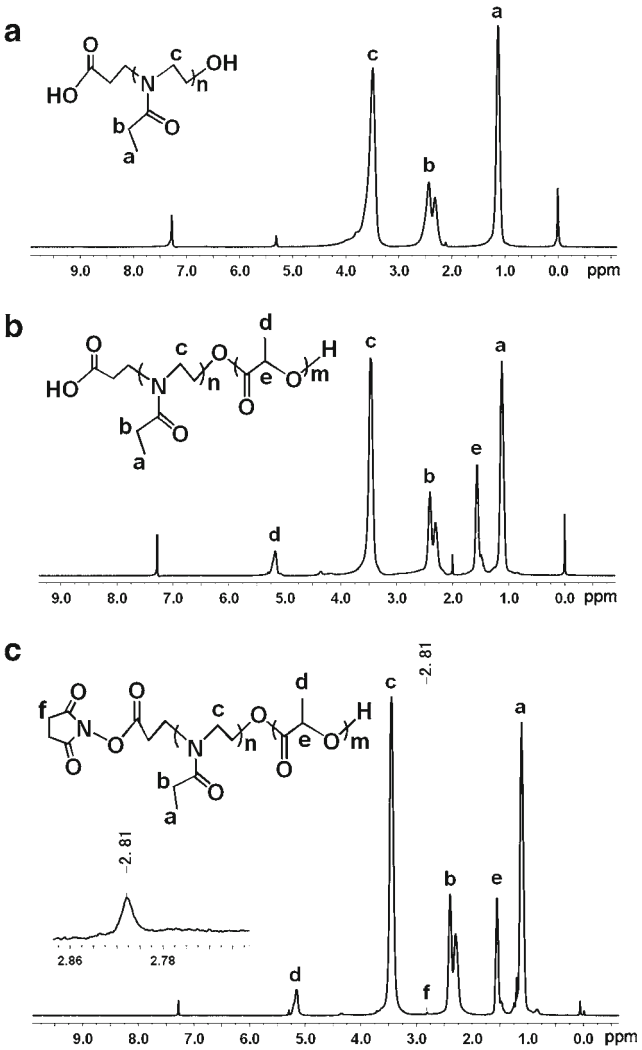

Fig. 3 ^{1}H-NMR spectrum of HOOC-PEOz-OH (**a**), HOOC-PEOz-PLA (**b**) and NHS-PEOz-PLA (**c**) in $CDCl_3$.

probe. The synthesized HOOC-PEOz-PLA exhibited a low CMC of 5.0 mg/L, indicating that the micelles formed by HOOC-PEOz-PLA might provide relatively high stability in systemic circulation as drug delivery carriers.

Synthesis and Characterization of NHS-PEOz-PLA and cRGDyK-PEOz-PLA

In order to conjugate cRGDyK and YPSMA-1 with HOOC-PEOz-PLA, HOOC-PEOz-PLA copolymer was first activated with NHS (Fig. 2b), which was confirmed by ^{1}H NMR (Fig. 3c). The presence of the characteristic resonances of NHS at 2.81 ppm indicated the successful conjugation of NHS to the terminal of HOOC-PEOz-PLA.

The conjugation of cRGDyK with NHS-PEOz-PLA was confirmed by HPLC analysis based on the decrease of the amount of cRGDyK (data not shown). The conjugation efficiency was about 47%.

Characterization of PM

The physicochemical characteristics of nanoparticles play an important role in determining their fate after administration (36). As listed in Table I, the synthesized HOOC-PEOz-PLA could self-assemble into micelles with a small average diameter of about 24 nm (blank micelles) and a narrow distribution determined by DLS. A slightly appreciable increase in size was observed for PTX-loaded micelles, implying a favorable stability of the nanocarriers. Furthermore, PTX-loaded PM modified with ligands was comparable in size to each other, indicating that the ligand conjugation did not affect the size of the micelles. Importantly, the size of these micelles was beneficial for a passive targeting delivery of drugs to tumors since they were small enough to penetrate through the leaky tumor vasculatures via EPR effect (37, 38), while reducing reticuloendothelial system (RES)-mediated clearance, and big enough to avoid renal filtration (36). In addition, the TEM images showed that the PMs were generally in spherical shape with good monodispersity (Fig. 4a and b). Furthermore, PTX-loaded micelles exhibited negative Zeta potential, which might be attributed to the carboxyl groups on the micelle surface. The micelles displayed higher drug encapsulation efficiency (EE) of >91% and loading content (LC) of >8.3%, which are crucial for their clinical application.

The *in vitro* release of PTX from various micelles at 37°C was evaluated using a dialysis method at pH 7.4 that mimics the blood environment. Moreover, the release profiles of PTX-loaded micelles under endo/lysosome mimetic circumstances (pH 5.0) were also investigated, since the delivery system would be trapped inside the endo/lysosomes after being endocytosed by tumor cells. As anticipated, the release of PTX from the micelles was pH-dependent. As presented in Fig. 4c–f, PTX showed a significantly slower release for all micelles at pH 7.4 compared with that at pH 5.0, and about 70% of PTX was leaked from the micelles within 24 h, while the release of PTX was accelerated at pH 5.0, and more than 97% of PTX escaped from the micelles within 24 h. Specifically, at 8 h, the release of PTX from four kinds of micelles was suppressed at pH 7.4 and the release profile reached a plateau with accumulative release of approximately 62.4, 64.9, 72.7 and 68.6% for PTX/PM, PTX/PM-R, PTX/PM-Y and PTX/PM-RY, respectively. In comparison, at pH 5.0, the release of PTX burst to approximately 88.8, 86.9, 87.1 and 89.3% at 8 h, respectively, and the release was sustained thereafter. Notably, the release of the micelles at pH 7.4 seemed high, which might be attributed to being accelerated by the solubilization of Tween 80 present in release medium. This release behavior of PMs in the case of our experiment was highly advantageous to targeted cancer therapy since the

Table I Physicochemical characteristics of blank micelles and various drug-loaded micelles ($n = 3$)

Polymeric micelles	Diameter (nm)	PDI	Zeta potential (mV)	EE (%)	LC (%)
Blank micelles	24.6 ± 0.9	0.15 ± 0.01	–	–	–
PTX/PM	28.3 ± 0.9	0.21 ± 0.01	−9.0 ± 0.2	98.78 ± 1.00	8.98 ± 0.09
PTX/PM-R	28.7 ± 1.5	0.24 ± 0.01	−18.1 ± 0.3	95.97 ± 0.15	8.72 ± 0.01
PTX/PM-Y	29.9 ± 1.4	0.26 ± 0.03	−2.0 ± 0.7	91.63 ± 0.98	8.33 ± 0.09
PTX/PM-RY	30.2 ± 0.6	0.24 ± 0.01	−3.8 ± 0.6	97.11 ± 0.42	8.83 ± 0.04
C6/PM	34.9 ± 0.4	0.22 ± 0.01	–	84.32 ± 3.63	–
C6/PM-R	33.9 ± 0.7	0.23 ± 0.01	–	89.86 ± 5.20	–
C6/PM-Y	37.3 ± 0.4	0.25 ± 0.01	–	81.43 ± 3.98	–
C6/PM-RY	64.7 ± 2.0	0.26 ± 0.03	–	87.15 ± 4.42	–

amount of drug released prematurely might be minimized during circulation in the bloodstream, thereby providing an enough amount of drug to effectively kill the cancer cells once the micelles were internalized via endocytosis.

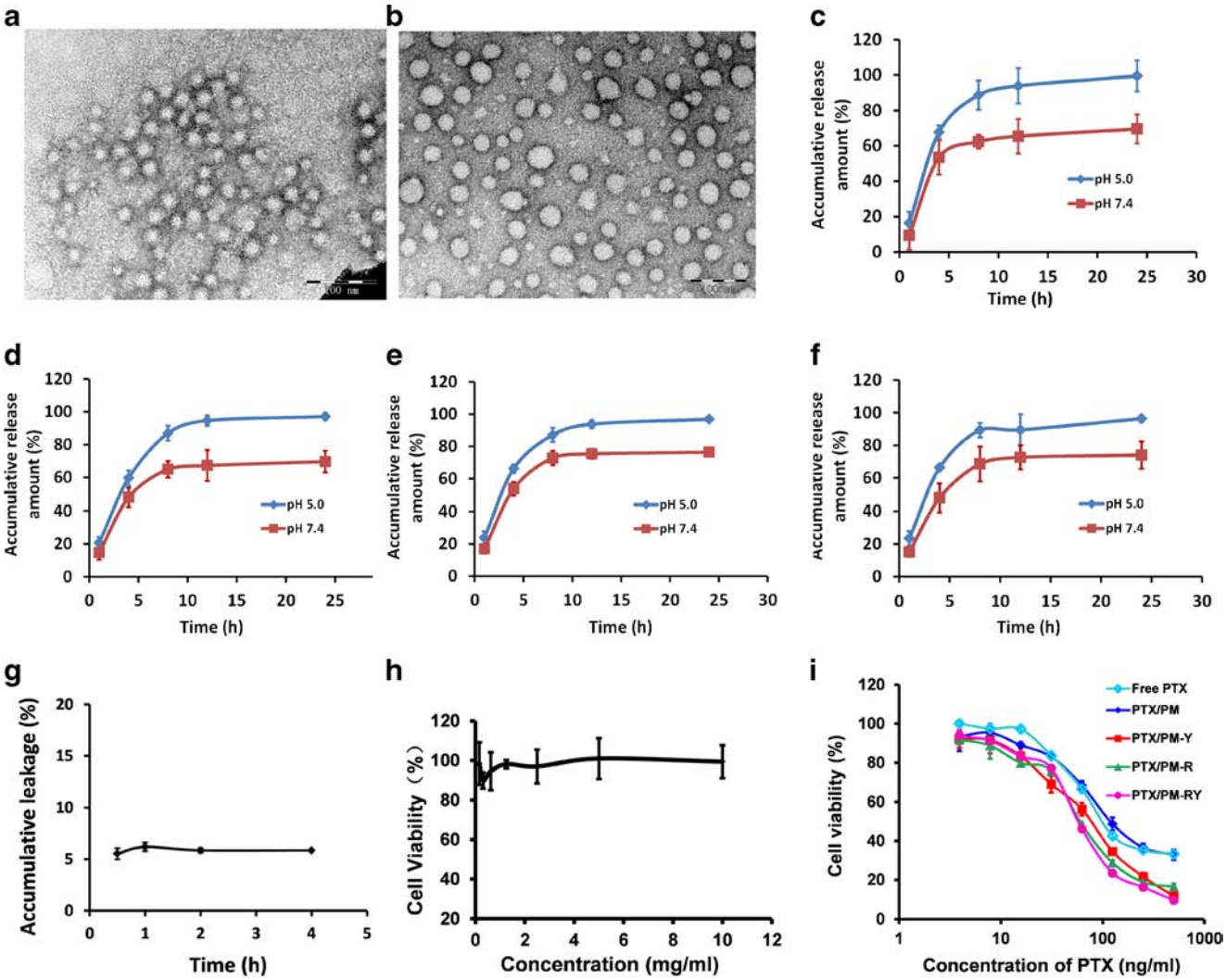

Fig. 4 TEM images of PTX/PM (**a**) and PTX/PM-RY (**b**). *In vitro* release profiles of PTX from PTX/PM (**c**), PTX/PM-R (**d**), PTX/PM-Y (**e**) and PTX/PM-RY (**f**) in PBS with different pH values at 37°C ($n = 3$). (**g**) *In vitro* leakage of C6 from PEOz-PLA micelles in serum-free medium for 4 h at 37°C ($n = 3$). Cytotoxicity of blank micelles (**h**) and various PTX-loaded micelles (**i**) against 22Rv1 cells after incubation for 72 h ($n = 6$). Scale bar is 100 nm.

To study the cellular uptake and intracellular distribution of our prepared micelles, a poorly water-soluble fluorescent probe C6 was loaded. As shown in Table I, the encapsulation efficiencies were all higher than 81%. The leakage profile of C6 from the representative micelles C6/PM in serum-free medium was shown in Fig. 4g. Up to 4 h, the leakage of C6 was less than 5.9% in total. These implied that the leaked C6 before the micelles contacted with the cells was negligible, and the behavior of C6 could represent the micelles.

Stability of PM After Contacting with Cells

FRET method was used to detect whether the core-loaded lipophilic agent is still encapsulated in the core of micelles when the micelles are in contact with cells. A FRET pair DiI/DiO was physically loaded into the inner core of PEOz-PLA micelles (denoted as FRET micelles) with an average diameter of 41.7±0.7 nm measured by DLS. If the FRET pair is located in the inner core of micelles, DiO is excited at a wavelength of 484 nm, the DiI will emit fluorescence at 565 nm. That is to say, FRET occurs due to the close proximity (<10 nm) of DiI and DiO. Upon release of the FRET pair from micelles, the distance between the FRET pair increased (>10 nm), resulting in decreased emission at 565 nm and increased emission at 501 nm (34).

As shown in Fig. 5a, FRET effect was clearly observed when FRET micelles were dispersed in deionized water. Thus, the prepared FRET micelles could be used to measure the FRET effect to monitor the encapsulation of the core-loaded molecules in micelles. Further, the confocal images showed that the FRET micelles outside 22Rv1 cells still had a strong FRET phenomenon (Fig. 5b), indicating that DiO and DiI could be closely retained inside the core of the micelles when FRET micelles incubated with 22Rv1 cells at the initial time. Thus, the behavior of the loaded C6 was considered representative of the behavior of micelles after they contacted with cells.

In Vitro Cytotoxicity

Biocompatibility is a great concern for biomaterials and in this study a preliminary evaluation of the cytotoxicity of the blank micelles was performed using SRB assay. 22Rv1 cells were chosen for this study because 22Rv1 cells are both integrin $\alpha_v\beta_3$- and PSMA-positive cells. A relative cell viability of around 100% was observed for 22Rv1 cells up to the highest polymer concentration of 10 mg/mL (Fig. 4h), and no significant change was detected in cell viability with increasing of copolymer concentration ($p>0.05$). These suggested that neither the HOOC-PEOz-PLA copolymer itself nor its hydrolytic products affected cell metabolism substantially. Eventually, HOOC-PEOz-PLA prepared in the present study was biocompatible, and was a good micelle-forming biomaterial for drug delivery.

To apply PTX-loaded micelles for therapy of cancer, their inhibiting effect on the growth of 22Rv1 cells was quantitatively evaluated *in vitro*, and the IC_{50} value (the drug concentration at which 50% of cells are killed) was calculated simultaneously. Apparent growth inhibition on 22Rv1 cells was observed in a concentration and formulation-dependent pattern (Fig. 4i). Free PTX could be internalized easily and accumulated in cells at high level, thus leading to high

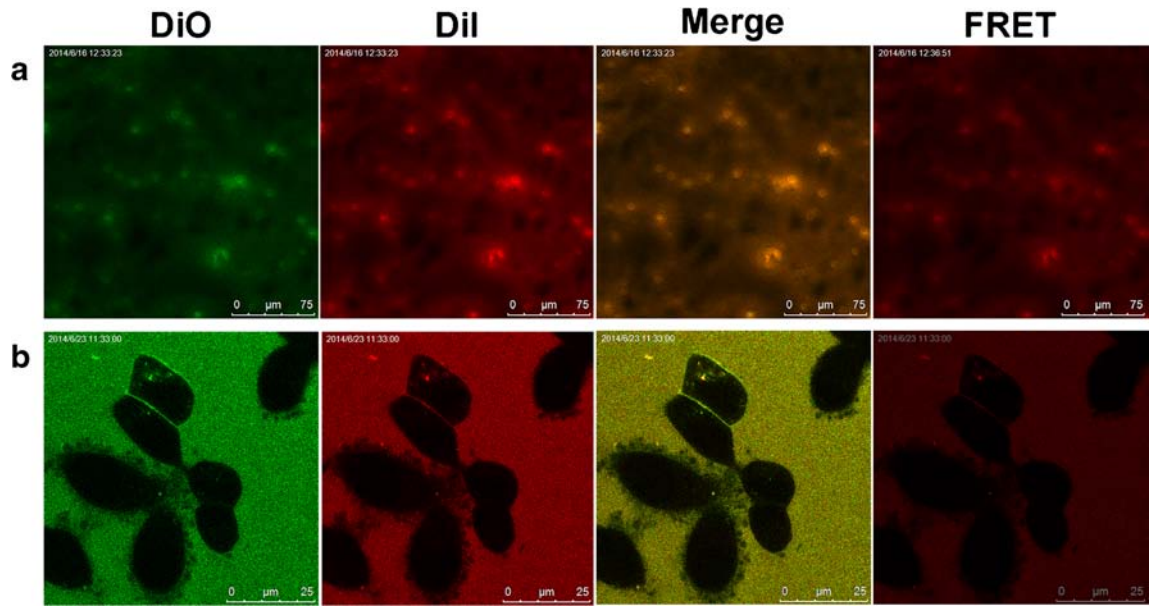

Fig. 5 (**a**) Confocal images of FRET micelles in deionized water. (**b**) Confocal images of FRET micelles incubated with 22Rv1 cells for 0.5 h. The Ex/Em of the DiO and DiI lines was DiO/DiO, DiI/DiI (484/501, 549/565). The Ex/Em of the FRET line was DiO/DiI (484/565). The *merge line* represents the fluorescence intensity.

cytotoxicity. The encapsulation of PTX into unmodified micelles (i.e., PTX/PM) resulted in no obvious increase in the cytotoxicity of PTX compared with free PTX, and the IC_{50} value of PTX/PM (70.56 ± 7.06 ng/mL) was comparative to that of free PTX (66.28 ± 3.85 ng/mL) ($p > 0.05$). As expected, the growth of tumor cells was severely inhibited by PTX/PM-RY, PTX/PM-Y and PTX/PM-R compared with that of PTX/PM, and the IC_{50} value of PTX/PM-RY (55.05 ± 3.47 ng/mL), PTX/PM-Y (64.04 ± 3.28 ng/mL) and PTX/PM-R (56.15 ± 4.74 ng/mL) was 1.28-, 1.10- and 1.26-fold lower than that of PTX/PM, respectively, suggesting that the conjugation of ligands to the surface of PTX/PM could increase the cytotoxicity of PTX against 22Rv1 cells, a both integrin $\alpha_v\beta_3$-overexpressing and PSMA-positive cell line. This superior cytotoxicity of ligands-modified micelles might be attributed to the cRGDyK and YPSMA-1 receptor targeting. Additionally, no significant difference in IC_{50} value was observed between PTX/PM-RY and PTX/PM-R ($p > 0.05$), whereas there existed significant difference in IC_{50} value between PTX/PM-RY and PTX/PM-Y ($p < 0.01$). The difference in cytotoxicity of ligand-modified PMs might be due to the difference in their cellular uptake as described below.

In Vitro Cellular Uptake

Flow cytometry was first utilized to quantitatively evaluate the cellular uptake of various C6-loaded micelles by 22Rv1 cells. C6 was employed as the marker for intracellular tracing. As shown in Figs. 6a and b, C6/PM-RY showed the highest cellular uptake, and the intracellular fluorescence intensity for C6/PM-RY was 2.74-, 1.77- and 1.37-fold higher than that for C6/PM, C6/PM-Y and C6/PM-R, respectively. These might benefit from both integrin $\alpha_v\beta_3$- and PSMA-mediated endocytosis. To prove this, the competitive inhibition of free cRGDyK or YPSMA-1 was assayed by incubation of free cRGDyK or YPSMA-1 with cells in advance. For preincubation of cRGDyK, the uptake of C6/PM-R could be significantly inhibited (Figs. 6c and d) ($p < 0.001$). Similar results were obtained for preincubation of YPSMA-1 for YPSMA-1-modified micelles. These confirmed that the enhanced cellular uptake of ligand-modified micelles was due to the mediation of dual receptors. Notably, the uptake of C6/PM-R was more than that of C6/PM-Y, which might be due to the difference in the expression amount of integrin $\alpha_v\beta_3$ and PSMA in cells or in the conjugation efficiency of cRGDyK and YPSMA-1.

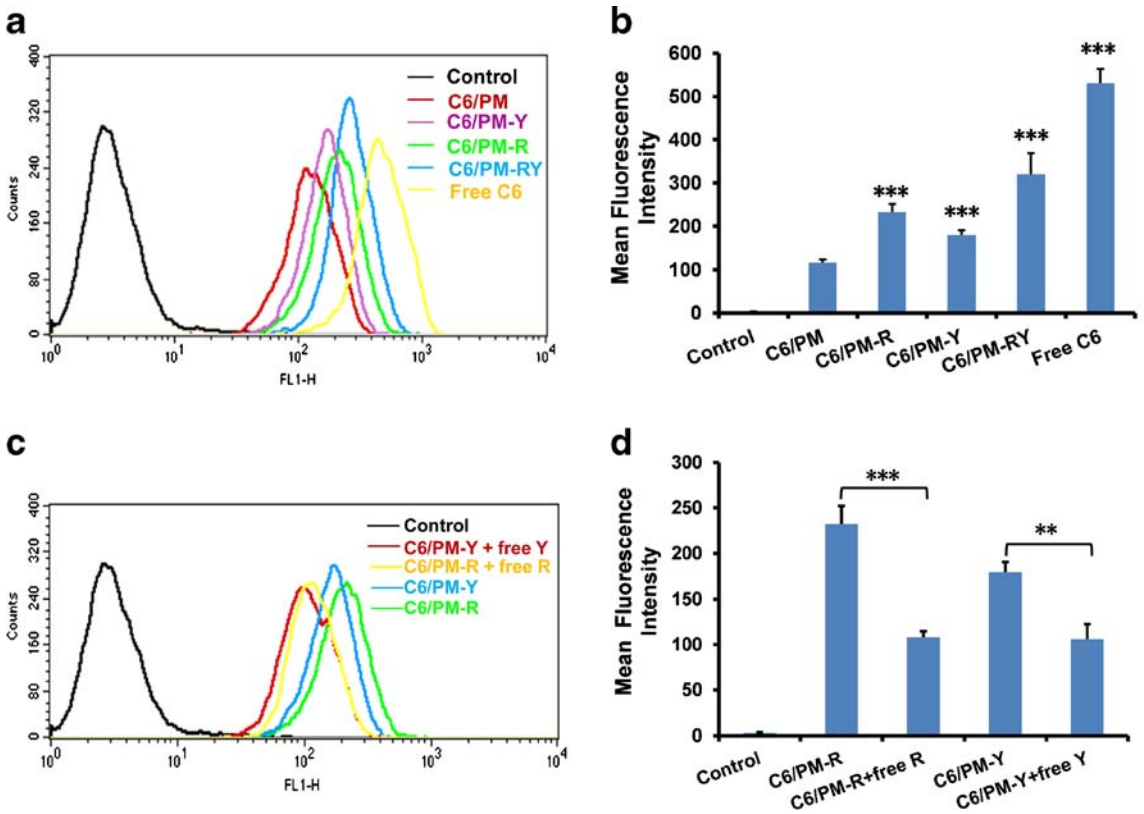

Fig. 6 (**a** and **b**) Quantitative flow cytometry analysis results of C6 uptake from various C6-loaded micelles by 22Rv1 cells after 4 h incubation. (**c** and **d**) The competitive inhibition of free cRGDyK and YPSMA-1 on C6 uptake by preincubation with 0.5 μg/mL of free cRGDyK and 0.1 μg/mL of free YPSMA-1 for 30 min, respectively, before 22Rv1 cells were exposed to the corresponding micelles. $^{**}p < 0.01$, $^{***}p < 0.001$ compared with the respective control. The final C6 concentration in each formulation was 100 ng/mL.

The cellular uptake was further visualized by CLSM to qualitatively evaluate the amount of micelles endocytosed by 22Rv1 cells and intracellular distribution using C6 as fluorescent probe. After being incubated with various C6 formulations for 1.5 h, 22Rv1 cells were fixed and stained with Hoechst 33258 to reveal their cell nuclei morphology *in vitro*. Figure 7 presented the intracellular accumulation and distribution of various C6 formulations in 22Rv1 cells. Because of its higher hydrophobicity, free C6 readily partitioned into the lipid membranes, thus leading to the most intense intracellular green fluorescence, and free C6 was mainly located in the cytoplasm. Further, CLSM observation demonstrated that the internalized micelles with green fluorescence and/or released C6 from the internalized micelles were also mainly located in the cytoplasm. Notably, the images showed a more intense green fluorescence in cells for C6/PM-RY, C6/PM-Y and C6/PM-R compared with C6/PM. As expected, cells treated with C6/PM-RY exhibited more intense green fluorescence than those treated with C6/PM-R and C6/PM-Y, respectively. Notably, the enhanced cellular uptake of C6/PM-R was obviously higher than that of C6/PM-Y, which were in agreement with the results obtained by flow cytometry, likely due to the conjugation efficiency of cRGDyK to micelles was higher than that of YPSMA-1. On the other hand, the level of PSMA expression in 22Rv1 cells might be lower than that of integrin $\alpha_v\beta_3$, and/or, there existed weaker specific interaction of YPSMA-1 with PSMA compared with that of cRGDyK with integrin $\alpha_v\beta_3$. These need to be further confirmed in future studies.

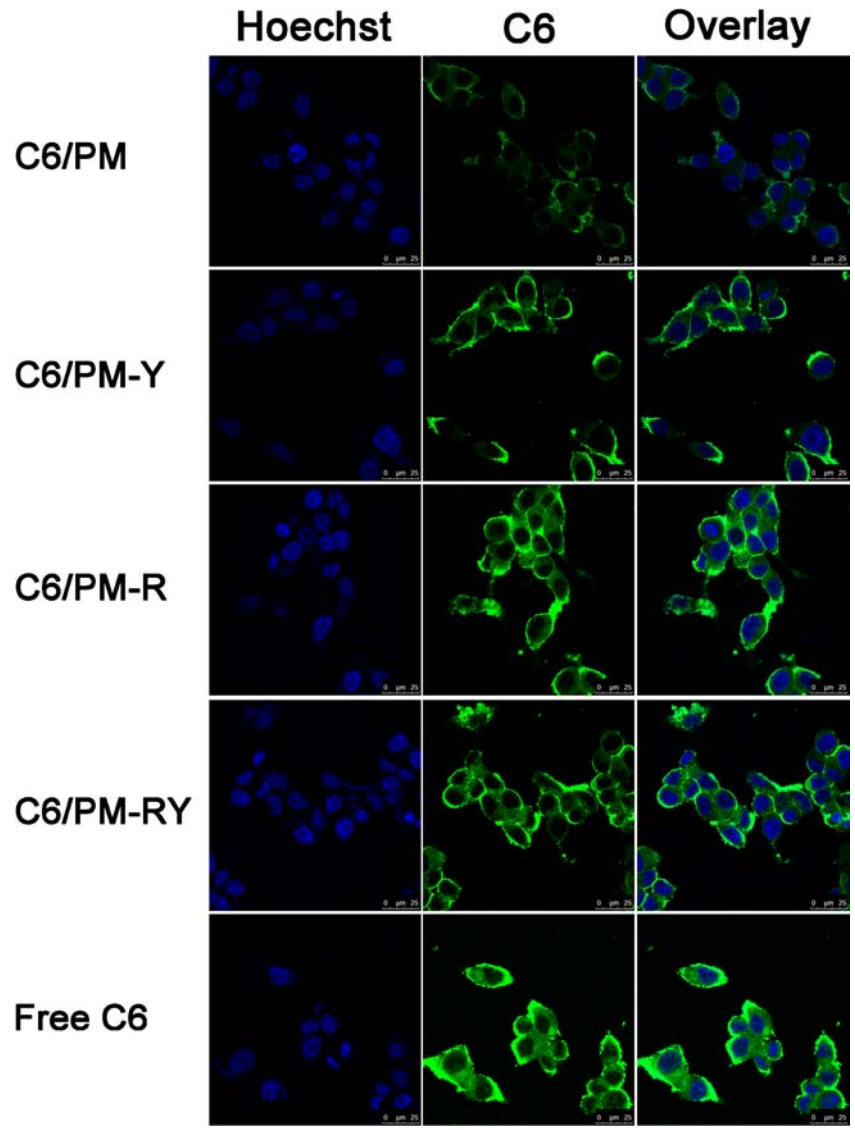

Fig. 7 CLSM images of 22Rv1 cells incubated with various C6 formulations at 37°C for 1.5 h. The final C6 concentration in each formulation was 50 ng/mL. Cell nuclei were stained blue with Hoechst 33258, and green fluorescence is from C6 encapsulated in micelles.

DISCUSSION

Formulating drugs to bind to the desired cellular targets is a necessary step in the design of anticancer drug delivery systems (39, 40). Further, following internalization, it is desirable to protect drugs from the degradation in the acidic lysosomes by the lysosome enzymes (24, 41). Introducing pH-sensitive moieties into the targeting drug delivery systems could achieve precise targetability and enhanced cellular internalization (42, 43), and quick endo/lysosome escape (44). Here, we developed novel dual-targeting pH-sensitive PM for collaboratively targeted delivery of PTX to tumors and explored their therapeutic efficiency for prostate cancer.

First, the diblock copolymer HOOC-PEOz-PLA was successfully synthesized and selected as the main micelle-forming material, and its biocompatibility with negligible cell cytotoxicity was confirmed (Fig. 4h). The synthesized HOOC-PEOz-PLA could self-assemble into micelles with a small diameter and narrow distribution in aqueous medium and high drug loading capacity (Table I). In addition, the combination of cRGDyK-PEOz-PLA with YPSMA-1-PEOz-PLA were engineered, which comprised the micelles for targeted delivery of PTX to tumor cells and controlled release triggered by endocytic pH after being internalized into tumor cells via endocytosis and trapped in acidic endocytic compartments, thus the toxicity of encapsulated PTX is made more tumor cell-specific and enhanced (43). As expected, the designed micelles in the present study distinguished endo/lysosome pH from physiological pH by accelerating drug release (Fig. 4c–f). This pH-dependent release was attributed to the peculiar structure of PEOz located in the outer shell of the micelles. In our previous work, the pK_a of PEOz-PLA was determined to be around 6.9. When pH value in the environment is lower than pK_a of PEOz-PLA, the amide groups of PEOz were ionized (45), thus leading to electrostatic repulsion between PEOz blocks which may induce the loose micelle structure (46) (Fig. 1a). Based on the *in vitro* release results, it could be concluded that after internalization of the micelles, pH-triggered drug release at endo/lysosome pH, which resulted in the "proton-sponge effect" and further led to the rupture of endo/lysosome membrane (47), could facilitate the escape of the micelles and their payload from endo/lysosomes. This pH-triggered quick drug release might remarkably enhance the intracellular free drug concentration in a short time (1, 48), being beneficial to kill tumor cells and shrink tumors (49) and possibly deterring the occurrence of drug resistance for tumor cells.

For effective cancer treatment, anticancer drug must be accumulated in tumors. One of the rational and effective strategies is to deliver drug to tumors using targeting ligand-modified nanocarriers (6, 16, 19, 30). Additionally, tumor cells typically overexpress multiple surface receptors that can mediate delivery of drug-loaded nanocarriers. However, most receptors are not exclusively expressed on tumor cells but also on some normal cells, and high affinity of targeted nanocarriers may lead to non-desired accumulation in regions of the body associated with low expression. Hence, for practical purposes, multi ligands-modified nanocarriers might exhibit better targetability (9, 10). As a proof-of-principle study, we have demonstrated the fabrication and characterization of a dual-ligand targeted system exploiting integrin $\alpha_v\beta_3$ and PSMA as target receptors to deliver PTX-loaded PM to prostate cancer cells 22Rv1 overexpressing both integrin $\alpha_v\beta_3$ and PSMA. The cellular uptake (Figs. 6a, b and 7), *in vitro* antitumor efficacy (Fig. 4i) provided strong evidences that dual-ligand-modified micelles could collaboratively and efficiently home to 22Rv1 tumors compared with single ligand-modified micelles, further demonstrating that the dual-ligand-modified micelle system was more efficient in delivering PTX to integrin $\alpha_v\beta_3$-rich and PSMA-expressed tumor cells than the corresponding single ligand-modified micelle systems, and suggesting the benefits of using dual-ligand-modified pH-sensitive micelles for collaboratively enhanced targeting ability and receptor-mediated cellular uptake (42, 43). Additionally, active targetability and pH-sensitivity could provide a synergistic effect, which was confirmed by *in vitro* antitumor effect results (Fig. 4i) (43). Overall, these results strongly supported our hypothesis that the application of combining dual-ligand-modification with pH-sensitivity to PM remarkably enhanced tumor cell recognition, promoted the cellular uptake, facilitated intracellular drug release, thereby improving the antitumor efficacy. The studies regarding *in vivo* antitumor efficacy will be carried out in near future to fully characterize the nature of dual-ligand-modified pH-sensitive micelles. In a word, the design concept in this study might provide a reference to the delivery of antitumor agents for safe and effective therapy of integrin $\alpha_v\beta_3$ and PSMA expressing prostate cancers.

CONCLUSION

In summary, dual-ligand-modified micelles in the present study had excellent performance featured by nano-scaled size, favorable pH-sensitivity to promote drug release in tumor cells, high integrin-binding and PSMA-binding affinity to collaboratively enhance targeting to tumor cells, leading to enhanced cellular uptake and thereby cytotoxicity. These suggested that dual-ligand-modified pH-sensitive drug delivery system might be a powerful drug carrier for targeting therapy of prostate cancers.

ACKNOWLEDGMENTS AND DISCLOSURES

This work was financially supported by the National Natural Science Foundation of China (No. 81172990), the National

Key Science Research Program of China (973 Program, 2015CB932100) and the Innovation Team of Ministry of Education (No. BMU20110263).

REFERENCES

1. Cui C, Xue YN, Wu M, Zhang Y, Yu P, Liu L, *et al.* Cellular uptake, intracellular trafficking, and antitumor efficacy of doxorubicin-loaded reduction-sensitive micelles. Biomaterials. 2013;34:3858–69.
2. Talelli M, Iman M, Varkouhi AK, Rijcken CJ, Schiffelers RM, Etrych T, *et al.* Core-crosslinked polymeric micelles with controlled release of covalently entrapped doxorubicin. Biomaterials. 2010;31:7797–804.
3. Yang X, Grailer JJ, Pilla S, Steeber DA, Gong S. Tumor-targeting, pH-responsive, and stable unimolecular micelles as drug nanocarriers for targeted cancer therapy. Bioconjug Chem. 2010;21:496–504.
4. Li X, Huang Y, Chen X, Zhou Y, Zhang Y, Li P, *et al.* Self-assembly and characterization of Pluronic P105 micelles for liver-targeted delivery of silybin. J Drug Target. 2009;17:739–50.
5. Wang F, Li X, Zhou Y, Zhang Y, Chen X, Yang J, *et al.* Nanoscaled polyion complex micelles for targeted delivery of recombinant hirudin to platelets based on cationic copolymer. Mol Pharm. 2010;7:718–26.
6. Moffattand S, Cristiano RJ. PEGylated J591 mAb loaded in PLGA-PEG-PLGA tri-block copolymer for targeted delivery: *in vitro* evaluation in human prostate cancer cells. Int J Pharm. 2006;317:10–3.
7. Allen TM. Ligand-targeted therapeutics in anticancer therapy. Nat Rev Cancer. 2002;2:750–63.
8. Muro S. Challenges in design and characterization of ligand-targeted drug delivery systems. J Control Release. 2012;164:125–37.
9. Bhattacharyya S, Khan JA, Curran GL, Robertson JD, Bhattacharya R, Mukherjee P. Efficient delivery of gold nanoparticles by dual receptor targeting. Adv Mater. 2011;23:5034–8.
10. Li X, Zhou H, Yang L, Du G, Pai-Panandiker AS, Huang X, *et al.* Enhancement of cell recognition *in vitro* by dual-ligand cancer targeting gold nanoparticles. Biomaterials. 2011;32:2540–5.
11. Hillier SM, Kern AM, Maresca KP, Marquis JC, Eckelman WC, Joyal JL, *et al.* 123I-MIP-1072, a small-molecule inhibitor of prostate-specific membrane antigen, is effective at monitoring tumor response to taxane therapy. J Nucl Med. 2011;52:1087–93.
12. Ikegami S, Yamakami K, Ono T, Sato M, Suzuki S, Yoshimura I, *et al.* Targeting gene therapy for prostate cancer cells by liposomes complexed with anti-prostate-specific membrane antigen monoclonal antibody. Hum Gene Ther. 2006;17:997–1005.
13. Bacich DJ, Pinto JT, Tong WP, Heston WD. Cloning, expression, genomic localization, and enzymatic activities of the mouse homolog of prostate-specific membrane antigen/NAALADase/folate hydrolase. Mamm Genome. 2001;12:117–23.
14. Wright GL, Grob Jr BM, Haley C, Grossman K, Newhall K, Petrylak D, *et al.* Upregulation of prostate-specific membrane antigen after androgen-deprivationtherapy. Urology. 1996;48:326–34.
15. Slovin SF. Targeting novel antigens for prostate cancer treatment: focus on prostate-specific membrane antigen. Expert Opin Ther Targets. 2005;9:561–70.
16. Sawant RM, Cohen MB, Torchilin VP, Rokhlin OW. Prostate cancer-specific monoclonal antibody 5D4 significantly enhances the cytotoxicity of doxorubicin-loaded liposomes against target cells *in vitro*. J Drug Target. 2008;16:601–4.
17. Yin J, Li Z, Yang T, Wang J, Zhang X, Zhang Q. Cyclic RGDyK conjugation facilitates intracellular drug delivery of polymeric micelles to integrin-overexpressing tumor cells and neovasculature. J Drug Target. 2011;19:25–36.
18. Eldar-Boock A, Miller K, Sanchis J, Lupu R, Vicent MJ, Satchi-Fainaro R. Integrin-assisted drug delivery of nano-scaled polymer therapeutics bearing paclitaxel. Biomaterials. 2011;32:3862–74.
19. Jiang X, Sha X, Xin H, Chen L, Gao X, Wang X, *et al.* Self-aggregated pegylated poly (trimethylene carbonate) nanoparticles decorated with c(RGDyK) peptide for targeted paclitaxel delivery to integrin-rich tumors. Biomaterials. 2011;32:9457–69.
20. Chen X, Plasencia C, Hou Y, Neamati N. Synthesis and biological evaluation of dimeric RGD peptide-paclitaxel conjugate as a model for integrin-targeted drug delivery. J Med Chem. 2005;48:1098–106.
21. Hambley TW, Hait WN. Is anticancer drug development heading in the right direction? Cancer Res. 2009;69:1259–62.
22. Torchilin V. Multifunctional and stimuli-sensitive pharmaceutical nanocarriers. Eur J Pharm Biopharm. 2009;71:431–44.
23. Klaikherd A, Nagamani C, Thayumanavan S. Multi-stimuli sensitive amphiphilic block copolymer assemblies. J Am Chem Soc. 2009;131:4830–8.
24. Sakai-Kato K, Un K, Nanjo K, Nishiyama N, Kusuhara H, Kataoka K, *et al.* Elucidating the molecular mechanism for the intracellular trafficking and fate of block copolymer micelles and their components. Biomaterials. 2014;35:1347–58.
25. Kim D, Lee ES, Oh KT, Gao ZG, Bae YH. Doxorubicin-loaded polymeric micelle overcomes multidrug resistance of cancer by double-targeting folate receptor and early endosomal pH. Small. 2008;4:2043–50.
26. Kim D, Gao ZG, Lee ES, Bae YH. *In vivo* evaluation of doxorubicin-loaded polymeric micelles targeting folate receptors and early endosomal pH in drug-resistant ovarian cancer. Mol Pharm. 2009;6:1353–62.
27. Zalipsky S, Hansen CB, Oaks JM, Allen TM. Evaluation of blood clearance rates and biodistribution of poly(2-oxazoline)-grafted liposomes. J Pharm Sci. 1996;85:133–7.
28. Wang X, Li X, Li Y, Zhou Y, Fan C, Li W, *et al.* Synthesis, characterization and biocompatibility of poly(2-ethyl-2-oxazoline)-poly(D, L-lactide)-poly(2-ethyl-2-oxazoline) hydrogels. Acta Biomater. 2011;7:4149–59.
29. Farokhzad OC, Cheng J, Teply BA, Sherifi I, Jon S, Kantoff PW, *et al.* Targeted nanoparticle-aptamer bioconjugates for cancer chemotherapy *in vivo*. Proc Natl Acad Sci U S A. 2006;103:6315–20.
30. Cheng J, Teply BA, Sherifi I, Sung J, Luther G, Gu FX, *et al.* Formulation of functionalized PLGA-PEG nanoparticles for *in vivo* targeted drug delivery. Biomaterials. 2007;28:869–76.
31. Li X, Yang Z, Yang K, Zhou Y, Chen X, Zhang Y, *et al.* Self-assembled polymeric micellar nanoparticles as nanocarriers for poorly soluble anticancer drug ethaselen. Nanoscale Res Lett. 2009;4:1502–11.
32. Zhang Y, Li X, Zhou Y, Fan Y, Wang X, Huang Y, *et al.* Cyclosporin A-loaded poly(ethylene glycol)-b-poly(d, l-lactic acid) micelles: preparation, *in vitro* and *in vivo* characterization and transport mechanism across the intestinal barrier. Mol Pharm. 2010;7:1169–82.
33. Li X, Li P, Zhang Y, Zhou Y, Chen X, Huang Y, *et al.* Novel mixed polymeric micelles for enhancing delivery of anticancer drug and overcoming multidrug resistance in tumor cell lines simultaneously. Pharm Res. 2010;27:1498–511.
34. Chen H, Kim S, Li L, Wang S, Park K, Cheng JX. Release of hydrophobic molecules from polymer micelles into cell membranes revealed by Forster resonance energy transfer imaging. Proc Natl Acad Sci U S A. 2008;105:6596–601.
35. Li N, Li XR, Zhou YX, Li WJ, Zhao Y, Ma SJ, *et al.* The use of polyion complex micelles to enhance the oral delivery of salmon calcitonin and transport mechanism across the intestinal epithelial barrier. Biomaterials. 2012;33:8881–92.
36. Duanand X, Li Y. Physicochemical characteristics of nanoparticles affect circulation, biodistribution, cellular internalization, and trafficking. Small. 2013;9:1521–32.
37. Maedaand H, Matsumura Y. Tumoritropic and lymphotropic principles of macromolecular drugs. Crit Rev Ther Drug Carrier Syst. 1989;6:193–210.

38. Gao ZG, Lukyanov AN, Singhal A, Torchilin VP. Diacyllipid-polymer micelles as nanocarriers for poorly soluble anticancer drugs. Nano Lett. 2002;2:979–82.
39. Liu C, Liu F, Feng L, Li M, Zhang J, Zhang N. The targeted co-delivery of DNA and doxorubicin to tumor cells via multifunctional PEI-PEG based nanoparticles. Biomaterials. 2013;34:2547–64.
40. Xiao Y, Hong H, Javadi A, Engle JW, Xu W, Yang Y, *et al.* Multifunctional unimolecular micelles for cancer-targeted drug delivery and positron emission tomography imaging. Biomaterials. 2012;33:3071–82.
41. Nam HY, Kwon SM, Chung H, Lee SY, Kwon SH, Jeon H, *et al.* Cellular uptake mechanism and intracellular fate of hydrophobically modified glycol chitosan nanoparticles. J Control Release. 2009;135: 259–67.
42. Hsiue GH, Wang CH, Lo CL, Wang CH, Li JP, Yang JL. Environmental-sensitive micelles based on poly(2-ethyl-2-oxazoline)-b-poly(L-lactide) diblock copolymer for application in drug delivery. Int J Pharm. 2006;317:69–75.
43. Wu H, Zhu L, Torchilin VP. pH-sensitive poly(histidine)-PEG/DSPE-PEG co-polymer micelles for cytosolic drug delivery. Biomaterials. 2013;34:1213–22.
44. Wang M, Hu H, Sun Y, Qiu L, Zhang J, Guan G, *et al.* A pH-sensitive gene deliverysystem based on folic acid-PEG-chitosan - PAMAM-plasmid DNA complexes for cancer cell targeting. Biomaterials. 2013;34:10120–32.
45. Wang CH, Hsiue GH. Synthesis and characterization of temperature- and pH-sensitive hydrogels based on poly(2-ethyl-2-oxazoline) and poly(D, L-lactide). J Polym Sci A Polym Chem. 2002;40:1112–21.
46. Zhang CY, Yang YQ, Huang TX, Zhao B, Guo XD, Wang JF, *et al.* Self-assembled pH-responsive MPEG-b-(PLA-co-PAE) block copolymer micelles for anticancer drug delivery. Biomaterials. 2012;33:6273–83.
47. Hu Y, Litwin T, Nagaraja AR, Kwong B, Katz J, Watson N, *et al.* Cytosolic delivery of membrane-impermeable molecules in dendritic cells using pH-responsive core-shell nanoparticles. Nano Lett. 2007;7:3056–64.
48. Xu GK, Feng XQ, Li B, Gao H. Controlled release and assembly of drug nanoparticles via pH-responsive polymeric micelles: a theoretical study. J Phys Chem B. 2012;116:6003–9.
49. Wang CH, Wang CH, Hsiue GH. Polymeric micelles with a pH-responsive structure as intracellular drug carriers. J Control Release. 2005;108:140–9.